Single-Station Contactless Respiration Detection Based on Wi-Fi CSI

Zhehan Liu
School of Electronic Engineering and Optical Engineering
Nanjing University of Science and Technology
Nanjing, China
zhehanliu@njust.edu.cn

Min Wu
Innovation Academy for Microsatellites of Chinese Academy of Sciences
Shanghai, China
m15000336722@163.com

Jun Zou
School of Electronic Engineering and Optical Engineering
Nanjing University of Science and Technology
Nanjing, China
jun_zou@njust.edu.cn

Guangzu Liu*
School of Electronic Engineering and Optical Engineering
Nanjing University of Science and Technology
Nanjing, China
liuguangzu@njust.edu.cn

***Abstract*—Real-time health monitoring is receiving increasing attention in both medical and consumer applications. To address the limitations of contact-based monitoring devices, various contactless monitoring methods have been explored. Wi-Fi-based integrated sensing and communication (ISAC) has emerged as a promising solution. However, most prior studies rely on commodity Wi-Fi devices and bistatic configurations, which introduce hardware dependency and limited deployment flexibility. In this paper, we investigate the feasibility of contactless respiration detection in a monostatic setup. Leveraging a software-defined radio (SDR) platform and open-source openwifi project with a pair of transmit and receive antennas, the system can extract Channel State Information (CSI) from its self-transmitted signals. A respiration detection method based on the Fresnel zone model is proposed. Experiments using a computer numerical control (CNC)-controlled reflector to simulate thoracic motion demonstrate the accuracy of the proposed frequency estimation method.**

Keywords—Wi-Fi sensing, CSI, Fresnel Zone, single-station, SDR, openwifi

I. INTRODUCTION

As environmental pollution worsens, the incidence of respiratory diseases rises, leading to a growing demand for real-time monitoring of respiratory rates in areas such as athletic recovery, medical supervision, and health assessment [1].

Traditional respiratory monitoring devices, such as chest belts and electrode patches, are costly and labor-intensive, requiring professional operation. Moreover, physical direct contact with the body can lead to discomfort or potential safety hazards, especially during overnight operation when power supply or charging is necessary [2].

Recognizing these challenges, researchers have conducted extensive studies on contactless monitoring methods. For instance, frequency modulated continuous wave millimeter-wave radar employs high-frequency electromagnetic waves to detect thoracic motion patterns [3], visible and infrared cameras, combined with artificial intelligence perform image-based respiratory recognition [4], and highly sensitive microphone arrays capture acoustic signals to infer breathing patterns.

Wi-Fi devices have gained considerable attention from researchers due to their ubiquity in smartphones, homes, and office environments [5] among these technologies. By leveraging Wi-Fi received signal strength or CSI, researchers have made significant progress in numerous research areas, including human presence detection, activity and gesture recognition, identification, localization, tracking, indoor positioning, fall detection [6]. A new IEEE Task Group, 802.11bf, is currently working on adapting the 802.11 Media Access Control and Physical (PHY) layer standards for Wi-Fi sensing purposes [7].

Almost all existing studies are based on commodity devices, tools such as the Intel 5300 CSI Tool, Atheros CSI Tool, Nexmon CSI Tool, and ESP32 CSI Tool are among the most popular platforms for obtaining CSI data [6]. These tools extract CSI information by modifying corresponding firmware or drivers, but they often suffer from hardware dependency, complex installation, and unstable performance. Furthermore, due to the limitations of commodity Wi-Fi devices, most studies adopt a bistatic base setup. In real-world environments such as homes, it is uncommon to deploy two fixed-position Wi-Fi routers, making this setup assumption less realistic.

This paper investigates the feasibility of contactless human respiration detection in a single-station setup and proposes a frequency estimation method based on the Fresnel Zone and open-source openwifi project. This paper also details the CSI extraction process implemented on the FPGA and other advantages of the single-station configuration. Experimental results demonstrate the effectiveness of the proposed method, offering valuable insights for router design and Wi-Fi sensing applications.

II. SYSTEM MODEL

A. Channel State Information(CSI)

In Wi-Fi communication systems, the PHY layer employs Orthogonal Frequency Division Multiplexing (OFDM)

modulation, which modulates digital symbols across multiple subcarriers. The Physical Protocol Data Unit (PPDU) frame header includes a series of pre-defined training symbols X, known as preambles, which are used by the receiver for signal acquisition and synchronization. Once the receiver successfully detects and extracts the preamble Y, it can perform channel estimation to derive the Channel Frequency Response(CFR)

$$Y(f) = H(f)X(f) + N \tag{1}$$

Where f is the frequency of certain subcarrier, N is the noise vector, H is the channel frequency response matrix, consisting of channel information from multiple subcarriers, commonly referred to as CSI.

$$H_{M\times N\times K\times T} = \begin{bmatrix} H_{m,n,1,1} & H_{m,n,1,2} & \cdots & H_{m,n,1,t} \\ H_{m,n,2,1} & H_{m,n,2,2} & \cdots & H_{m,n,2,t} \\ \vdots & \vdots & \ddots & \vdots \\ H_{m,n,k,1} & H_{m,n,k,2} & \cdots & H_{m,n,k,t} \end{bmatrix}, m \in [0,M], n \in [0,N] \tag{2}$$

Considering a Multiple-Input Multiple-Output (MIMO) channel, H is a series of complex matrices with M transmit antennas, N receive antennas and K subcarriers. CSI characterizes the propagation properties of wireless signals over the communication link, capturing effects such as reflection, diffraction, fading, and distortions introduced by internal circuit components. Each CSI element includes both amplitude and phase information, and the use of multiple subcarriers enables a fine-grained representation of the CFR. In practical Wi-Fi systems, CSI estimation is affected by factors such as multipath propagation, signal processing at both the transmitter and receiver, and imperfections in hardware and software. The estimated baseband CSI between a given transmit antenna and receive antenna can be expressed as:

$$H(k,\tau_n) = (\sum_{n}^{N} \alpha_n e^{-j2\pi\tau_n f_k}) e^{-j2\pi\varepsilon f_k t} e^{-j2\pi\rho f_k} e^{-j2\pi\eta f_k} \tag{3}$$

Where N represents the number of multipaths between the transmitter and receiver, α_n and τ_n denote the amplitude attenuation and propagation delay of the signal for the N_{th} path respectively. f_k is the frequency of k_{th} subcarrier, ε represents the normalized Carrier Frequency Offset(CFO) error, ρ represents the normalized Sampling Time Offset (STO) error, and η represents the normalized Sampling Frequency Offset (SFO) error. Furthermore, since the introduction of MIMO in 802.11n, additional factors such as Cyclic Shift Diversity and beamforming techniques can also introduce changes in amplitude and phase.

B. Fresnel zone Sensing Model

While binary and multi-class classification applications usually use learning-based methods, almost all the estimation applications use modeling-based algorithms including but not limited to Doppler Spread, Power Delay Profile, Root-MUSIC and Fresnel zone model.

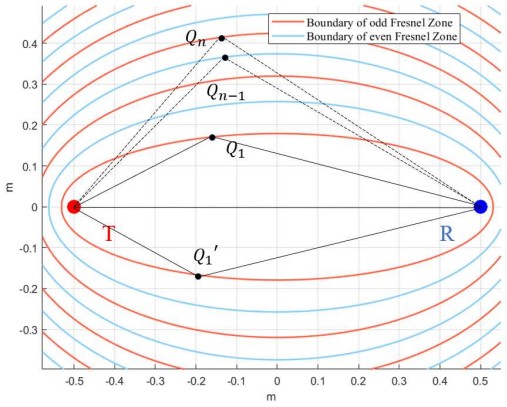

Fig. 1. Fresnel zone model with 1m focal separation at 2412 MHz

The concept of Fresnel zone originates from the Augustin Fresnel's research on the interference and diffraction of light. In the context of Wi-Fi sensing, the Fresnel zone model was first introduced by Zhang[8], practical experiments have demonstrated that this theoretical framework effectively elucidates the relationship between human motion and received signals.

The boundaries of the Fresnel zones are defined as a series of concentric ellipsoids, with the transmitter and receiver as their focal points shown in Fig. 1. At a given wavelength λ, the boundary of the nth Fresnel Zone is defined by a concentric ellipsoid that satisfies the corresponding equation:

$$b_n = \{Q_n, |Q_nT| + |Q_nR| - |TR| = n\lambda/2\} \tag{4}$$

Where Q_n is a point in the nth ellipse, T and R are two transceivers at same height. When $n = 1$, the reflected signal has a longer propagation path compared to the line-of-sight (LOS) transmission by $\lambda/2$, resulting in a phase rotation of π. Additionally, the half-wavelength loss introduces a phase jump of π, causing the reflected signal to have the same phase with the LOS signal. This leads to amplitude addition and an increase in signal strength. When $n = 2$, the reflected signal 's phase becomes opposite to the LOS signal, resulting in amplitude subtraction and a decrease in signal strength. This phenomenon is reflected in the CSI, where the amplitude of the subcarrier corresponding to that frequency exhibits a corresponding change. As n increases, the strength of the superposed signal exhibits periodic fluctuations.

Moreover, chest movements during respiration are subtle, typically ranging from 5 mm in shallow breathing to 12.6 mm in deep breathing [9], leading to a slight change in the reflected path length. At a carrier frequency of 2.4 GHz, such displacement corresponds to a phase rotation of less than 35 degrees, making detection challenging. To enhance the signal variation caused by such small motions, it is optimal to place the target near the center of the boundary between adjacent Fresnel zones, where exhibits the highest sensitivity to path length variations.

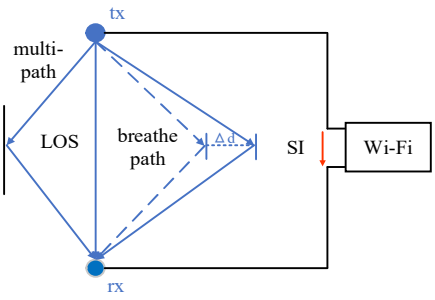

Fig. 2.Single-station sensing model with SI

III. SINGLE-STATION SETUP AND SDR

A. Single-Station Setup

While the Wi-Fi 7 standard is exploring the hybrid use of Time Division Duplexing (TDD) and Frequency Division Duplexing (FDD), most conventional Wi-Fi devices still operate in TDD mode. At any given frequency and time, a device can only either transmit or receive which means the receive channel is not active during transmission. This is why nearly all existing studies are based on a dual-station setup.

In the context of sensing, the capability to receive self-transmitted signals is particularly valuable. This allows the system to operate in a radar-like manner, making monostatic CSI sensing not only feasible but also advantageous in terms of enhancing user privacy.

Compared to the bistatic setup, the CSI estimated from a single-station configuration includes additional self-interference(SI), a phenomenon commonly observed in full-duplex systems. Following the power amplification, the transmitted signal may directly leak into the receiver chain. If the transmit and receive antennas are placed too closely, near-field coupling may also introduce significant SI into the receiving channel.

But moderate levels of SI generally do not hinder the proper demodulation of the received signal. And this interference is typically constant in stationary station setup. The overall Channel Impulse Responses (CIR) can be expressed as the superposition of multiple individual CIR components:

$$h(k,t,\tau) = h_{SI}(k,\tau) + h_{LOS}(k,\tau) + h_{mp}(k,\tau) + h_{dy}(k,t,\tau) \quad (5)$$

$$h(k,t,\tau) = h_{st}(k,\tau) + h_{dy}(k,t,\tau) \quad (6)$$

Where $h_{SI}(k,t)$ represents the self-interference component, $h_{LOS}(k,t)$ is the direct line-of-sight path, $h_{mp}(k,t)$ denotes the static multipath component and $h_d(k,t,\tau)$ captures the dynamic path variation caused by chest movement. The multipath variations caused by respiratory motion are inherently reflected in $h_d(k,t,\tau)$.

B. Hardware

SDR serves as a crucial tool for research in the fields of wireless communication and security. The SDR platform used in our experimental setup is based on the Xilinx XC7Z020-CLG400 + AD9361 RF agile transceiver architecture. The Zynq SoC core board runs the opensource openwifi project [10], which supports 802.11a/g/n protocols in AP, STA, monitor, and ad-hoc modes based on softmac architecture.

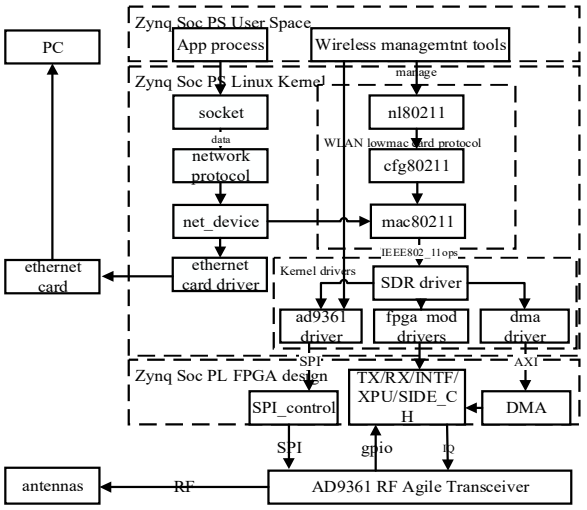

Fig. 3 Openwifi project structure

On the Zynq SoC platform, the Cortex ARM processor hosts an embedded Linux operating system, which primarily handles MAC layer control. FPGA's Programmable Logic side is programmed to implement the transceiver of Wi-Fi signal. Some logical control functions of distributed coordination function are also implemented within the FPGA. Subsequent tasks, such as filtering, ADC/DAC, up/down conversion, and AGC, are handled by the AD9361 agile transceiver chip.

There are two main differences between this SDR-based Wi-Fi device and commodity Wi-Fi.

First, special full-duplex mode. The AD9361 chip operates in FDD mode, the receive channel can remain continuously active while the transmit channel is in use which means the SDR board can receive signals sent by itself, such as periodically transmitted beacon signals.

Second, smaller CFO and SFO. The local RF clock and baseband clock for both the transmit and receive channels are derived from the same reference clock input. The frequency difference of clocks between transmit and receive channel is minimal. Therefore, the estimated CSI will be less affected by CFO and SFO which means the CSI information is more precise.

C. CSI Collection Algorithm

Due to differences in hardware circuitry and baseband processing algorithms across network cards from various manufacturers and models, even when receiving identical electromagnetic signals, the resulting CSI estimates can differ significantly.

The accuracy and resolution of CSI data can vary significantly across different devices, and variations in experimental environments further complicate the reproducibility and comparability of research in ISAC. Most existing CSI denoising and feature extraction methods typically operate on the CSI outputs provided by commercial devices,

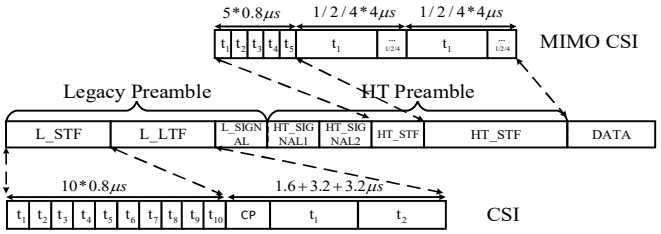

Fig. 4 802.11n HT-mixed mode PPDU frame structure

neglecting the signal distortions that may occur during earlier stages of signal processing. In contrast, SDR provides a fully transparent and customizable process from IQ samples to CSI, enabling more accurate and controllable CSI acquisition.

Fig. 4 illustrates the PPDU frame structure under the HT-mixed mode of the 802.11n protocol, which is the most widely supported standard among current Wi-Fi devices. The frame header, Legacy Short Training Field (L-STF) and Legacy Long Training Field (L-LTF) are present by all Wi-Fi devices for backward compatibility. The L-STF is composed of ten identical 16-sample repetitions. A commonly used approach exploits the repetitive nature of the L-STF for auto-correlation and cross-correlation calculations, which are also used for frequency offset estimation. Once the signal detection criteria are met, the presence of a signal is confirmed.

$$AutoCorr[i] = \frac{\| \sum_{i=0}^{N} S[i] * S^{*}[i+M] \|}{\sum_{i=0}^{N} S[i] * S^{*}[i]} \tag{7}$$

$$\hat{f}_{CFO} = angle(\frac{AutoCorr}{MT}) \tag{8}$$

$$CrossCorr[i] = \frac{\| \sum_{i=0}^{N} S[i] * L^{*}[i] \|}{\sum_{i=0}^{N} S[i] * S^{*}[i]} \tag{9}$$

Compared to the L-STF using only 12 subcarriers, the following L-LTF sequence is longer and uses 53 subcarriers, allowing for more accurate symbol timing and frequency offset estimation. After compensating the L-LTF using the estimated timing and frequency offset, the signal is demodulated to the frequency domain performing FFT, channel estimation algorithms can be applied to extract CSI from the L-LTF. For example, the widely used Least Squares method offers fast computation but lacks noise suppression, resulting in relatively large estimation errors.

$$\hat{H}_{LS} = \frac{Y}{X} \tag{10}$$

Beyond the L-LTF-based CSI extraction, the HT-mixed mode frame includes an HT Preamble after the Legacy Preamble, which provides richer CSI information across multiple antennas.

Fig. 5 provides a detailed depiction of the FPGA implementation flow for CSI computation in the openwifi project.

D. Respiration Detection Algorithm

A respiration detection method is applied to the CSI fluctuations to extract the desired respiratory information.

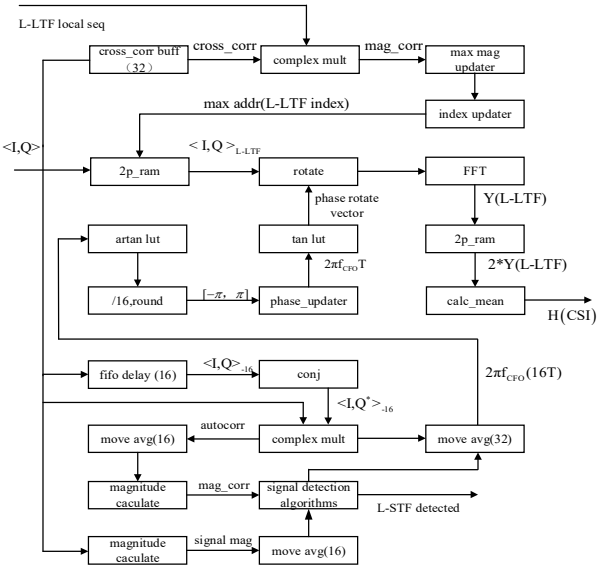

Fig. 5. Steps of CSI extraction in FPGA

1) Magnitude Calculation. Based on the Fresnel zone model, amplitude variations in CSI most directly reflect subtle chest movements rather than phase information which is often more susceptible to noise.

2) Outlier Removal. Environmental noise, electromagnetic interference, and hardware imperfections introduce anomalies in CSI sequence. A Hampel filter is employed to eliminate abrupt fluctuations that can distort respiration detection.

3) Noise Reduction. After removing outliers, residual noise still remains. A band-pass filtering centered on the expected respiration frequency range, or a wavelet transform is applied to further enhance signal clarity.

4) FFT. The filtered CSI amplitude sequence exhibits periodic fluctuations due to breathing. FFT is used to extract the dominant frequency component.

5) Subcarrier Selection. As CSI consists of multiple subcarriers, estimated frequencies from each are evaluated, spurious results are discarded, and the final respiration rate is determined by averaging valid subcarrier ones.

IV. Experiment Setup and Results

A. Experimental Setup

The experimental setup is illustrated in Fig. . A CNC machine drives a linear rail equipped with a plastic reflector(12cm*22cm), simulating chest movement by enabling precise reciprocating motion within a fixed range and at controllable frequencies. The SDR platform running the Openwifi project is connected to two vertically polarized omnidirectional 2.4 GHz antennas, each mounted on a tripod at a height of 75 cm, aligned with the height of the table and placed 1 m apart. One antenna serves as the transmitter and the other as the receiver. The system operates on Wi-Fi channel 1, with a center frequency of 2412 MHz, 20 MHz bandwidth, and a packet transmission rate of 10 packets per second, consistent

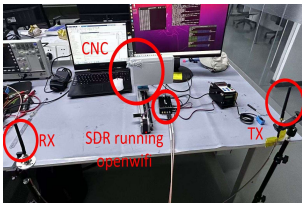

(a)CNC-controlled reflector, antenna, and SDR position

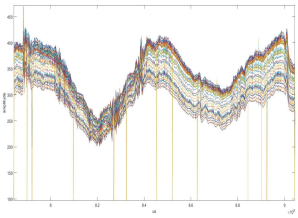

(b)CSI amplitude as reflector crosses the Fresnel Zone

Fig. 6.Experiment setup and validation result

with the standard Wi-Fi beacon frame interval. The reflector's motion is perpendicular to the LOS path between the antennas.

To validate the feasibility of the Fresnel Zone model under a single-station transceiver configuration, the CNC-controlled reflector was moved forward by 25 cm, starting from the boundary of the first Fresnel zone boundary. At the operating frequency, the theoretical minor axis lengths of the odd-order Fresnel zone boundaries are 17.90 cm, 31.93 cm, and 42.38 cm. As the reflector moves across multiple Fresnel zone boundaries, the CSI amplitude sequence exhibits a clear peak-valley-peak pattern showed in Fig. , thereby confirming the validity of the model.

B. Experimental Results

The CNC platform was configured to move with an amplitude of 12 mm, which approximates the displacement caused by deep human respiration. The movement frequencies were set to 0.2 Hz, 0.4 Hz, and 0.6 Hz, respectively. Due to the limited precision in stepper motor speed control and delays during direction switching, slight deviations from the target frequencies may occur.

The detected frequencies exhibit a clear harmonic relationship, and the estimated frequencies are highly accurate, with errors controlled within 3%. Accurate frequency estimation can also be achieved when using two directional antennas to monitor the movement of a distant CNC platform.

CONCLUSION

This paper investigates the feasibility of single-station contactless respiration detection using Wi-Fi CSI and SDR. By adopting the openwifi project, we address critical limitations of commodity Wi-Fi devices, including CFO/SFO instability and bistatic deployment constraints. The Fresnel zone model proves effective in guiding sensor placement for optimal sensitivity to sub-centimeter thoracic displacements. Experimental validation with a CNC-controlled reflector confirms the proposed accurate respiration rate estimation method. Future work will extend to multi-target scenarios and real-human trials. This paper offers a methodology reference for scalable, privacy-preserving health monitoring and informs next-generation standards for Wi-Fi sensing.

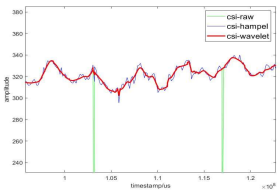

(a)CSI amplitude before and after signal processing

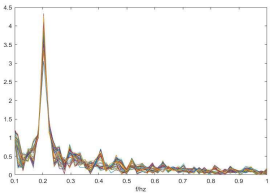

(b)Detection results during reflector reciprocating at 0.2Hz

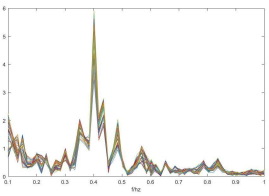

(c)Detection results during reflector reciprocating at 0.4Hz

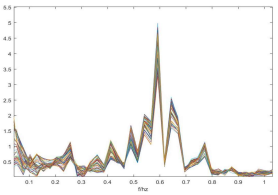

(d)Detection results during reflector reciprocating at 0.6Hz

Fig. 7.Experiment results of frequency estimation

REFERENCES

[1] Gambhir, Sanjiv Sam, T. Jessie Ge, Ophir Vermesh, and Ryan Spitler. "Toward achieving precision health." Science translational medicine,vol. 10, no. 430 eaao3612. Feb, 2018

[2] K. Verma, P. Preity and R. Ranjan, "An Insight into Wearable Devices for Smart Healthcare Technologies," 2023 13th International Conference on Cloud Computing, Data Science & Engineering, Noida, India, 2023, pp. 426-431.

[3] B. R. Upadhyay, A. B. Baral and M. Torlak, "Vital Sign Detection via Angular and Range Measurements With mmWave MIMO Radars: Algorithms and Trials," in *IEEE Access*, vol. 10, pp. 106017-106032, 2022.

[4] S. M. M. Islam, N. Molinaro, S. Silvestri, E. Schena and C. Massaroni, "Respiratory Feature Extraction for Contactless Breathing Pattern Recognition Using a Single Digital Camera," in IEEE Transactions on Human-Machine Systems, vol. 53, no. 3, pp. 642-651, June 2023.

[5] W. Zhao, H. Zhang, J. Zou, G. Liu and F. Shu, "Effective Chirp Modulation Communication System Design for LEO Satellite IoT," in IEEE Internet of Things Journal, vol. 12, no. 11, pp. 16962-16976, 1 June1, 2025

[6] Ma Y, Zhou G, Wang S. "WiFi sensing with channel state information: A survey, " ACM Computing Surveys (CSUR),vol. 52, no. 46, pp 1-36. June 2019.

[7] C. Chen, H. Song, Q. Li, F. Meneghello, F. Restuccia and C. Cordeiro, "Wi-Fi Sensing Based on IEEE 802.11bf," in IEEE Communications Magazine, vol. 61, no. 1, pp. 121-127, January 2023.

[8] H.Wang, D. Zhang, J. Ma, Y.Wang, Y.Wang and D. Wu. "Human respiration detection with commodity wifi devices: do user location and body orientation matter? " Proceedings of the 2016 ACM International Joint Conference on Pervasive and Ubiquitous Computing pp.25-36 September 2016.

[9] Lowanichkiattikul, C, Dhanachai, M, Sitathanee, C. "Impact of chest wall motion caused by respiration in adjuvant radiotherapy for postoperative breast cancer patients. "SpringerPlus 5, 144, 2016.

[10] X. Jiao, W. Liu, M. Mehari, M. Aslam and I. Moerman, "openwifi: a free and open-source IEEE802.11 SDR implementation on SoC," 2020 IEEE 91st Vehicular Technology Conference (VTC2020-Spring), Antwerp, Belgium, 2020, pp. 1-2